SRTTU

Journal of Electrical and Computer Engineering Innovations

JECEI, Vol. 3, No. 2, 2015

Regular Paper

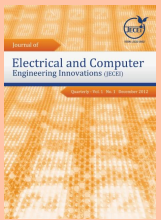

Modified Physical Optics Approximation for RCS Calculation of Electrically Large Objects with Coated Dielectric

Hossein Mohammadzadeh[1,*], Abolghasem Zeidaabadi-Nezhad[1], and Zaker Hossein Firouzeh[1]

[1]Department of Electrical and Computer Engineering, Isfahan University of Technology (IUT), Isfahan, Iran

*Corresponding Author's Information: h.mohammadzadeh@ec.iut.ac.ir

ARTICLE INFO

ARTICLE HISTORY:
Received 19 November 2015
Revised 22 December 2015
Accepted 27 December 2015

KEYWORDS:
Asymptotic techniques
Physical optics (PO)
Approximation
Radar cross section (RCS)
Coated objects
Modified PO

ABSTRACT

The Radar Cross Section of a target plays an important role in the detection of targets by radars. This paper presents a new method to predict the bistatic and monostatic RCS of coated electrically large objects. The bodies can be covered by lossy electric and/or magnetic Radar Absorbing Materials (RAMs). These materials can be approximated by the Fresnel reflection coefficients. The proposed method uses modified Physical Optics (PO) approximation to obtain the object scattered field. One of the advantages is the use of Stationary Phase Method (SPM) to solve the PO integral. This is becausethe SPM reduces significantly the computation time required to solve this integral as compared to rigorously numerical integration techniques. Simulationresults are presented to verify the accuracy and efficiency of the proposed method. The results are compared with commercial FEKO and CST software in order to show its superiority as far as the computation time is concerned.

1. INTRODUCTION

Radar Cross Section (RCS) of a target plays an important role in the detection of targets by radars. Recently, more efforts have been done to develop rigorous methods to analyze the RCS and radiation problems of electrically large objects such as aircrafts, satellites, terrestrial vehicles and ships [1]-[8]. Increasing or decreasing the RCS of an object is dependent upon the desired applications. In the past decades, two ways were usually used to reduce the RCS of objects, that is, the modification of the shape of objects and covering the bodies by radar absorbing materials (RAMs) [2]. Analysis of coated objects which are usually large compared with the wavelength, is generally a complicated problem. Numerical techniques such as Method of Moment (MoM), Finite Element Method (FEM) and Finite Difference Time Domain (FDTD) are used as solution methods [10]. These methods are efficient and flexible computational tools for the analysis of scattering and radiation electromagnetic problems, however, the main limitations of these methods are time-consuming and lengthy calculations. An extensive work has been done to increase the efficiency of the MoM [10]. For example, Multilevel Fast Multipole Method (MLFMM) only requires the storing of the near field terms of the coupling matrix, consequently reduces the computation time [10]. In addition, the objects with the dimensions of about 100 times of a wavelength can be analyzed by the MLFMM [1]. However, high frequency asymptotic techniques are widely used in large dimension problems of radiation and scattering due to their high efficiency compared with the MLFMM [9]. Since, the asymptotic approximation does not need to calculate the coupling matrix in contrast with the MLFMM [1]. One of the asymptotic techniques is Physical Optics (PO) approximation that broadly is used for PEC objects

and structures covered with lossy materials [1]-[3],[8]-[9],[11]. These materials can be approximated by the Fresnel reflection coefficients. However, the main drawback of the PO approximation is the lack of considering the edge and surface diffraction.

Hrer in, based on the PO approximation a modified method is presented to determine the induced surface current on the object bodies. This method allows to predict the bistatic and monostatic RCS of electrically large targets coated by RAMs. Also, the accuracy of the proposed method are illustrated by comparing the results with the results of FEKO and CST software. One of the advantages of the proposed method is the use of Stationary Phase Method (SPM) [12],[13] to solve the PO integrals. Because, the SPM reduces the computation time required to solve these integrals rather than numerical integration techniques used in other techniques [14]. The SPM is used to calculate the integrals of curved surface. In contrast, the Gaussian's method is used for flat surfaces [2],[14]. Efficiency of these methods have been proven for PEC objects [11],[14]. For the analysis of RCS problems by the Gaussian's method or SPM, theobjects are classified in three categories [2],[14]:

- Flat plates with all their points situated on the same plane.
- Single curved objects that are created by a set of straight lines (e.g. cylinder and conical surfaces).
- Double curved objects that are surfaces without any limitations (e.g. sphere).

The rest of the paper is organized as follows. The proposed method based on PO is described in Section 2. The scattering of electromagnetic waves from the finite cone is described in Section 3. The validity of the proposed method is examined in Section 4, where the results are compared with commercial FEKO and CST software. Concluding remarks are given in Section 5.

2. THE MODIFIED PHYSICAL OPTICS APPROXIMATION

Asymptotic techniques for solving electromagnetic problems such as Geometrical Optics (GO), Geometrical Theory of Diffraction (GTD), and Uniform Theory of Diffraction (UTD) based on rays include caustic problems. However, the current based methods such as Physical Optics (PO) and Physical Theory of Diffraction (PTD) can be used to overcome these problems [18]. In References [1]-[2] and [15], it is shown that the expression of electric and magnetic currents induced on the body of the object is as follows.

$$\mathbf{J}_s(\mathbf{r}') = \hat{n}\times\begin{bmatrix} 1+R_{\parallel} & 0 \\ 0 & 1-R_{\perp} \end{bmatrix}\begin{bmatrix} \mathbf{H}^i_{\parallel}(\mathbf{r}') \\ \mathbf{H}^i_{\perp}(\mathbf{r}') \end{bmatrix}\Bigg|_{\text{on } s'} \quad (1a)$$

$$\mathbf{M}_s(\mathbf{r}') = -\hat{n}\times\begin{bmatrix} 1+R_{\perp} & 0 \\ 0 & 1-R_{\parallel} \end{bmatrix}\begin{bmatrix} \mathbf{E}^i_{\perp}(\mathbf{r}') \\ \mathbf{E}^i_{\parallel}(\mathbf{r}') \end{bmatrix}\Bigg|_{\text{on } s'} \quad (1b)$$

Which $\hat{n}$ is the unit vector normal to the surface, s' is the surface of the object illuminated by the incident field and $R_{\parallel}$ and $R_{\perp}$ are the parallel and perpendicular components of the Fresnel reflection coefficients, respectively. However, there is a mistake in this approach. To find the distributed current usins this approach, it is assumed that the outer field of the dielectric is the total field. Due to the equivalent surface currents radiate in the vicinity of an object having electric field permittivity coefficient $\grave{o}_r$ and magnetic permeability coefficient μ_r, it is not therefore permitted to use Green's function of unbounded space in order to obtain radiation fields a companying the induced currents. In this paper, it is shown that accurate expressions for these currents, which are proven by the boundary conditions and image theory for large body, are as follows.

$$\mathbf{J}_s(\mathbf{r}') = 2\hat{n}\times\begin{bmatrix} R_{\parallel} & 0 \\ 0 & -R_{\perp} \end{bmatrix}\begin{bmatrix} \mathbf{H}^i_{\parallel}(\mathbf{r}') \\ \mathbf{H}^i_{\perp}(\mathbf{r}') \end{bmatrix}\Bigg|_{\text{on } s'} \quad (2a)$$

$$\mathbf{M}_s(\mathbf{r}') = 0 \quad (2b)$$

The above currents distribution reduces to well-known PO approximation for PEC case, that is $R_{\parallel}$ =+1 and $R_{\perp} = -1$. Consider a coated PEC object with thickness t, electric permittivity coefficient $\grave{o}_r$ and magnetic permeability coefficient μ_r as shown in Figs. 1 and 2.

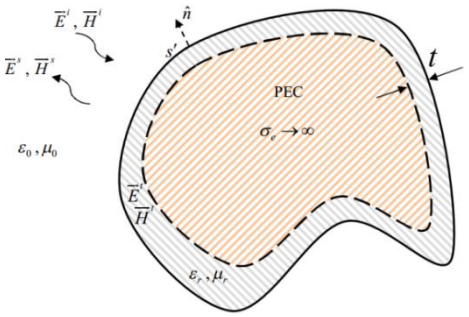

Figure 1: Incidence and reflection from a coated PEC objects.

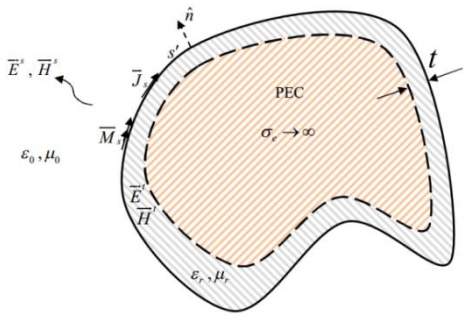

Figure 2: Induced currents at the boundary of a coated PEC object.

Using the boundary conditions for the induced electric and magnetic currents on the surface, we have:

$$\mathbf{J}_s(\mathbf{r}') = \hat{n}\times\left(\mathbf{H}^s - \mathbf{H}^t\right)\Big|_{\text{on s}'}$$

$$\mathbf{M}_s(\mathbf{r}') = -\hat{n}\times\left(\mathbf{E}^s - \mathbf{E}^t\right)\Big|_{\text{on s}'} \quad (3)$$

where $\mathbf{E}^t$ and $\mathbf{H}^t$, respectively, are electric and magnetic fields transmitted into the dielectric layer and $\mathbf{E}^s$ and $\mathbf{H}^s$ are scattered fields from the target, respectively.

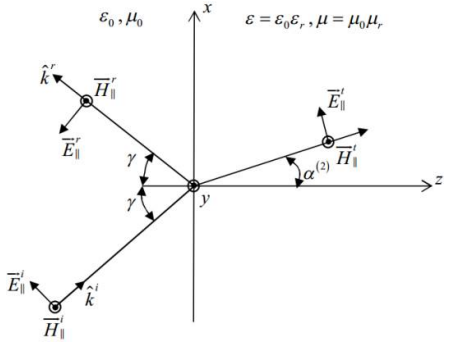

Figure 3: Incident, reflected and transmitted fields into the dielectric layer for parallel polarization case.

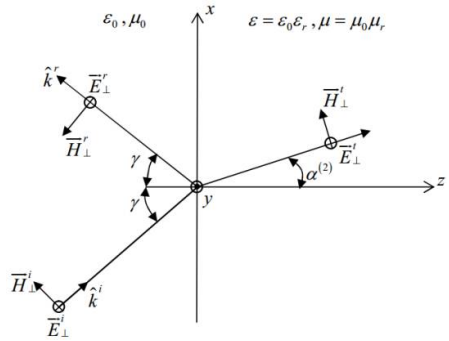

Figure 4: Incident, reflected and transmitted fields into the dielectric layer for perpendicular polarization case.

According to Fig. 3 for parallel polarization (or vertical polarization), surface currents $\mathbf{J}_s$ and $\mathbf{M}_s$ based on Fresnel transmission and reflection coefficients, can be written as (4), (5):

$$\begin{aligned}\mathbf{J}_{s\parallel}(\mathbf{r}') &= \hat{n}\times\left(\mathbf{H}_{\parallel}^s - \mathbf{H}_{\parallel}^t\right)\Big|_{\text{on s}'} \\ &= \hat{n}\times\left(R_{\parallel}\mathbf{H}_{\parallel}^i - T_{\parallel}\mathbf{H}_{\parallel}^i\right)\Big|_{\text{on s}'} \\ &= \left(R_{\parallel} - T_{\parallel}\right)\hat{n}\times\mathbf{H}_{\parallel}^i\Big|_{\text{on s}'}\end{aligned} \quad (4)$$

$$\begin{aligned}\mathbf{M}_{s\parallel}(\mathbf{r}') &= -\hat{n}\times\left(\mathbf{E}_{\parallel}^s - \mathbf{E}_{\parallel}^t\right)\Big|_{\text{on s}'} \\ &= -\hat{n}\times\left(R_{\parallel}\mathbf{E}_{\parallel}^i - T_{\parallel}\mathbf{E}_{\parallel}^i\right)\Big|_{\text{on s}'} \\ &= -\left(R_{\parallel} - T_{\parallel}\right)\hat{n}\times\mathbf{E}_{\parallel}^i\Big|_{\text{on s}'}\end{aligned} \quad (5)$$

Where $T_{\parallel}$ is the parallel component of the Fresnel transmitted coefficient. Note that the interior fields are not desired, so they can be equal to zero based on Love's principle (which is a result of the Stratton-Chu theorem) [18].

Hence, (4) and (5) can be reduced to the following forms:

$$\mathbf{J}_{s\parallel}(\mathbf{r}') = \hat{n}\times\mathbf{H}_{\parallel}^s\Big|_{on\ s'} = R_{\parallel}\hat{n}\times\mathbf{H}_{\parallel}^i\Big|_{\text{on s}'} \quad (6)$$

$$\mathbf{M}_{s\parallel}(\mathbf{r}') = -\hat{n}\times\mathbf{E}_{\parallel}^s\Big|_{on\ s'} = -R_{\parallel}\hat{n}\times\mathbf{E}_{\parallel}^i\Big|_{\text{on s}'} \quad (7)$$

Using Schelkunoff equivalence principle [18], the object is filled with PMC as shown in Fig. 5. Since the object is large compared to the wavelength, the image theory can be used to remove the object resulting in the surface currents that radiate into the unbounded space.

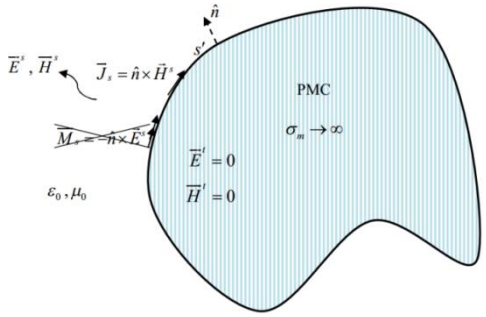

Figure 5: Zero field inside the dielectric coated object and remove one of the surface currents with filling it by PMC.

Therefore, the electric and magnetic surface currents in parallel polarization case are:

$$\mathbf{J}_{s\parallel}(\mathbf{r}') = 2R_{\parallel}\hat{n}\times\mathbf{H}_{\parallel}^i\Big|_{\text{on s}'} \quad (8a)$$

$$\mathbf{M}_{s\parallel}(\mathbf{r}') = 0 \quad (8b)$$

According to Fig. 4, if the previous process is used for the perpendicular polarization (or horizontal polarization) case, the equivalent surface currents are:

$$\mathbf{J}_{s\perp}(\mathbf{r}') = -2R_{\perp}\hat{n}\times\mathbf{H}_{\perp}^i\Big|_{\text{on s}'} \quad (9a)$$

$$\mathbf{M}_{s\perp}(\mathbf{r}') = 0 \quad (9b)$$

So, for the total currents $\mathbf{J}_s(\mathbf{r}')$ and $\mathbf{M}_s(\mathbf{r}')$, we have:

$$\mathbf{J}_s(\mathbf{r}') = 2\hat{n}\times\begin{bmatrix} R_{\parallel} & 0 \\ 0 & -R_{\perp}\end{bmatrix}\begin{bmatrix}\mathbf{H}_{\parallel}^i(\mathbf{r}') \\ \mathbf{H}_{\perp}^i(\mathbf{r}')\end{bmatrix}\Bigg|_{\text{on s}'} \quad (10a)$$

$$\mathbf{M}_s(\mathbf{r}') = 0 \tag{10b}$$

3. Scattering of Electromagnetic Waves from the Finite Cone

The geometry of the problem is a PEC cone with lower radius a, upper radius b and length L coated with a dielectric layer with thickness t coating all the surfaces. This geometry is depicted in Fig. 6. It is assumed that the radius of the object curvature is large compared to the wavelength. Also, the coating layer thickness should be small compared to the curvature radius. The scatterer is illuminated by a TM^z-polarized plane wave in incident angles θ_i, ϕ_i, given by

$$\mathbf{H}^i = \hat{\phi}_i H_0 e^{jk_0 \rho \sin\theta_i \cos(\phi - \phi_i)} e^{jk_0 z \cos\theta_i} \tag{11}$$

where,

$$\hat{\phi}_i = -\hat{x}\sin\phi_i + \hat{y}\cos\phi_i \tag{12}$$

and k_0 is the intrinsic wave number.

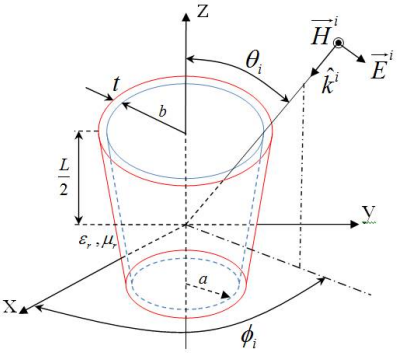

Figure 6: The geometry of the finite cone scatterer.

For a three-layered structure, air-dielectric-PEC, which is shown in Fig. 7, the expression for $R_{\parallel}$ and $R_{\perp}$ are given by [16], [19].

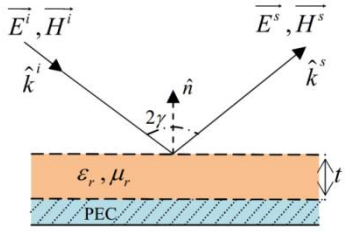

Figure 7: The geometry of the reflection.

$$R_{\parallel} = -\frac{Z_{i\parallel}^{(2)}\cos\alpha^{(2)} - \eta_0\cos\gamma}{Z_{i\parallel}^{(2)}\cos\alpha^{(2)} + \eta_0\cos\gamma} \tag{13}$$

$$R_{\perp} = \frac{Z_{i\perp}^{(2)}\cos\gamma - \eta_0\cos\alpha^{(2)}}{Z_{i\perp}^{(2)}\cos\gamma + \eta_0\cos\alpha^{(2)}} \tag{14}$$

where,

$$\cos\alpha^{(2)} = \sqrt{1-\left(1/\grave{o}_r\mu_r\right)\sin^2\gamma}$$
$$Z_{i\parallel}^{(2)} = Z_{i\perp}^{(2)} = jZ^{(2)}\tan\left(c^{(2)}t^{(2)}\right) \tag{15}$$

and,

$$Z^{(2)} = \eta_0\sqrt{\frac{\mu_r}{\grave{o}_r}} \quad , t^{(2)} = t$$
$$c^{(2)} = k_0\sqrt{\mu_r\grave{o}_r}\cos\alpha^{(2)} \tag{16}$$

which, the thickness of the dielectric layer is denoted by *t*, and $\eta_0 = \sqrt{\mu_0/\grave{o}_0}$ is the intrinsic impedance of free-space.

It should be noted that, these Fresnel coefficients are valid for flat surfaces. Since the body of the structure shown in Fig. 6 is curved, so the plane wave incident angle is different at each point of the object surface. Note that the body size is electrically large at the reflection point; consequently, the surface can be locally considered flat and Snell's law is valid as well[17].

Therefore, according to Fig. 8, to find a relationship between the reflection and incidence angles, and the angle of incident direction respect to the normal line at each point of the surface, the unit vector $\hat{n}$ in the Cartesian coordinate system is obtained as follows.

$$\mathbf{N} = \hat{\rho} - \left(\frac{b-a}{L}\right)\hat{z}$$
$$= \hat{x}\cos\phi + \hat{y}\sin\phi - \left(\frac{b-a}{L}\right)\hat{z} \tag{17}$$

and so

$$\hat{n} = \frac{\mathbf{N}}{|\mathbf{N}|} \tag{18}$$

As a result, the relationship between the angles of incident and reflected fields and the vector normal to the surface at each point of the surface is given by:

$$\cos\gamma = -\hat{k}^i\cdot\hat{n} = \frac{\hat{r}_i\cdot\left(\hat{x}\cos\phi+\hat{y}\sin\phi-\left(\frac{b-a}{L}\right)\hat{z}\right)}{|\mathbf{N}|}$$
$$= \left(\hat{x}\sin\theta_i\cos\phi_i+\hat{y}\sin\theta_i\sin\phi_i+\hat{z}\cos\theta_i\right)\cdot\frac{\left(\hat{x}\cos\phi+\hat{y}\sin\phi-\left(\frac{b-a}{L}\right)\hat{z}\right)}{|\mathbf{N}|}$$
$$= \frac{\sin\theta_i\cos(\phi-\phi_i)-\left(\frac{b-a}{L}\right)\cos\theta_i}{|\mathbf{N}|} \quad (19)$$

where

$$|\mathbf{N}| = \sqrt{1+\left(\frac{b-a}{L}\right)^2} \quad (20)$$

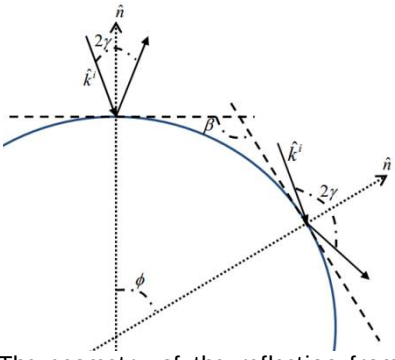

Figure 8: The geometry of the reflection from a curved surface.

By substitution of the (2a) into the expression of the magnetic vector potential [18], the scattered field from the finite cone is ultimately obtained as follows [18].

$$\mathbf{A}^s = \frac{\mu_0 e^{-jkr}}{4\pi r}\iint_{s'}\mathbf{J}_s(\mathbf{r}')e^{jkr'\cos\zeta}ds' \quad (21)$$

where

$$r'\cos\zeta = \rho'(z')\sin\theta\cos(\phi'-\phi)+z'\cos\theta \quad (22)$$

and for the cone, $\rho'(z')$ is as follow

$$\rho'(z') = \frac{b-a}{L}z'+a \quad (23)$$

and therefore

$$\mathbf{H}^s = \mathbf{H}_1^s + \begin{cases}\mathbf{H}_2^s & ;\theta_i<90\\ \mathbf{H}_3^s & ;\theta_i>90\end{cases} \quad (24)$$

which $\mathbf{A}^s$ is the magnetic vector potential and $\mathbf{H}_1^s$ is the scattered magnetic field from the body of the cone that is in range $\alpha<\theta_i<\alpha+180$ for $\alpha=\tan^{-1}((b-a)/L)$ and $\mathbf{H}_2^s$ and $\mathbf{H}_3^s$, respectively, are the scattered magnetic fields from the upper and lower plate of the cone. Therefore, the RCS is obtained as follows [18].

$$\sigma_{3D} = \lim_{r\to\infty}\left(4\pi r^2\frac{|\mathbf{H}^s|^2}{|\mathbf{H}^i|^2}\right) \quad (25)$$

which σ_{3D} is the three-dimensional radar cross section. To calculate the integral in (21) rapidly and accurately, the second order phase stationary method (SPM) is used as described in [2],[12]-[14] (especially in [12]).

4. Numerical Results

To show the effectivness of the proposed method, five cases are considered here. Firstly, the bistatic RCS of a PEC cylinder coated, as a special case of the cone structure, namely: $b=a$, with a low-loss dielectric, and with the radius of 2λ and the length of 4λ is obtained by the proposed method for both elevation and azimuth planes. The results are shown in Figs. 9 and 10. As shown, the dielectric characteristics are $\grave{o}_r=4$, $\tan\delta=0.25$ and $t=0.08\lambda$.

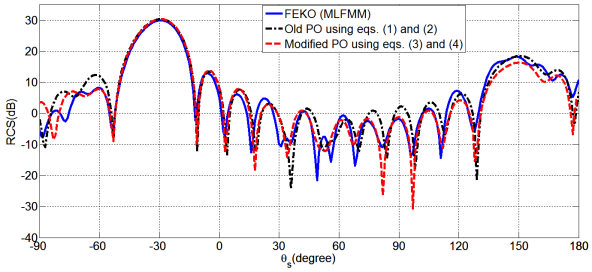

Figure 9: Bistatic RCS for the coated PEC cylinder (low-loss) in elevation plane with $\theta_i=30^\circ$, $\phi_i=0^\circ$ and $\phi_s=0^\circ$.

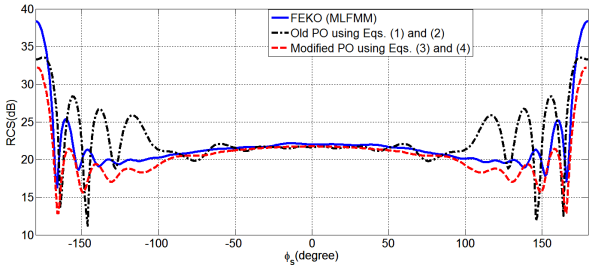

Figure 10: Bistatic RCS for the coated PEC cylinder (low-loss) in azimuth plane with $\theta_i=90^\circ$, $\phi_i=0^\circ$ and $\theta_s=90^\circ$.

The scatterer is illuminated by a TM^z-polarized plane wave with the angles of $\theta_i=30^\circ$ and $\phi_i=0^\circ$ in the spherical coordinates. Fig. 9 depicts the RCS in the elevation plane for $\phi_s=0^\circ$ and $-90^\circ\le\theta_s\le180^\circ$. This figure shows that the results of the elevation plane are

in good agreement with FEKO results obtained by MLFMM.

Fig. 10 shows the RCS in azimuth plane for $\theta_s = 90^\circ$ and $-180^\circ \le \phi_s \le 180^\circ$ when the scatterer is illuminated by a plane wave with the angles of $\theta_i = 90^\circ$ and $\phi_i = 0^\circ$. But in azimuth plane, beyond the range of $-100^\circ \le \phi_s \le 100^\circ$, the result shows little errors. Since the PO approximation is valid only for the illuminated region. Therefore, getting closer to the specular angle, more accurate results are obtained by the PO approximation. It is observed from Figs. 9 to 10 that the PO results are slightly different from the MLFMM results because of neglecting the edge and surface diffraction.

In the second case, the bistatic RCS of a PEC cylinder coated with a lossy dielectric is calculated as shown in Figs. 11 and 12. The radius and the length of the cylinder is 2λ and 4λ, respectively. The dielectric characteristics are $\grave{o}_r = 4$, $\tan\delta = 0.5$ and $t = 0.08\lambda$. Incident and scattered angles for the elevation and azimuth planes are the same as the first case. Figs. 11 and 12 show the RCS of coated cylinder in the elevation and azimuth planes, respectively. Figs. 11 and 12 show that the results of PO are different from the MLFMM results because of neglecting the edge and surface diffraction.

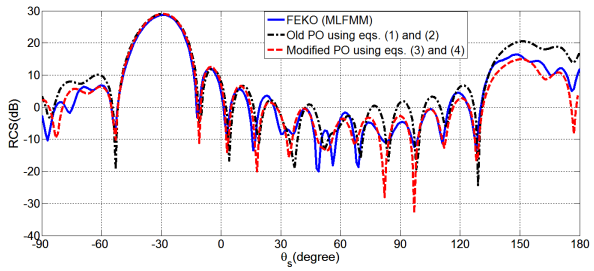

Figure 11: Bistatic RCS for the coated PEC cylinder in elevation plane that $\theta_i = 30^\circ$, $\phi_i = 0^\circ$ and $\phi_s = 0^\circ$.

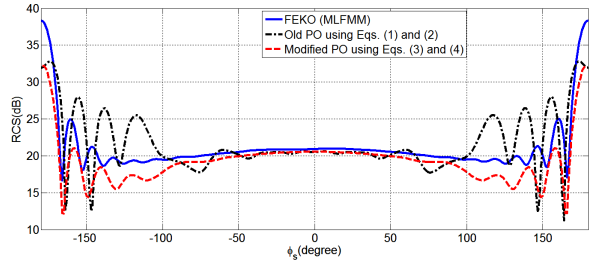

Figure 12: Bistatic RCS for the coated PEC cylinder in azimuth plane that $\theta_i = 90^\circ$, $\phi_i = 0^\circ$ and $\theta_s = 90^\circ$.

In the third case, the bistatic RCS of a PEC cylinder coated with a lossy dielectric is calculated as shown in Figs. 13 and 14.

The radius, length of the cylinder, dielectric characteristics and thickness of the dielectric are the same as the second case. However, the incident and scattered angles for the elevation and azimuth planes are different from the previous case. In this case the scatterer is illuminated by a TM^z-polarized plane wave with the angles of $\theta_i = 60^\circ$ and $\phi_i = 0^\circ$ for the elevation plane and $\theta_i = 45^\circ$ and $\phi_i = 0^\circ$ for the azimuth plane in the spherical coordinates.

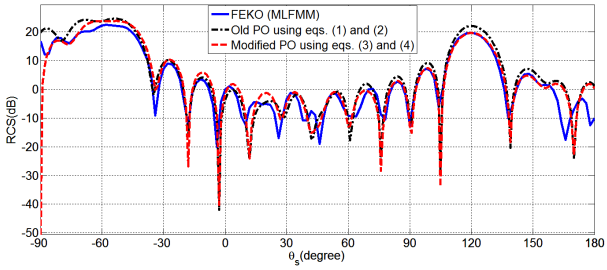

Figure 13: Bistatic RCS for the coated PEC cylinder in elevation plane that $\theta_i = 60^\circ$, $\phi_i = 0^\circ$ and $\phi_s = 0^\circ$.

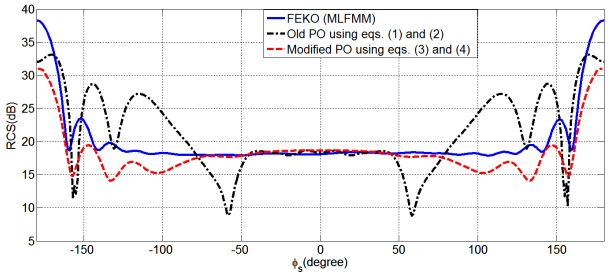

Figure 14: Bistatic RCS for the coated PEC cylinder in azimuth plane that $\theta_i = 45^\circ$, $\phi_i = 0^\circ$ and $\theta_s = 90^\circ$.

In the fourth case, the bistatic RCS of a PEC cone coated with a lossy dielectric and with the bottom radius of 2λ and the upper radius of 4λ and the length of 4λ is obtained by the proposed method for both elevation and azimuth planes.

The results are shown in Figs. 15 and 16. Also, in this case the dielectric characteristics are $\grave{o}_r = 4$, $\tan\delta = 0.25$ and $t = 0.08\lambda$.

Since the mesh size has to be very small for this case to simulate with the MoM and MLFMM methods leading to the much memory in FEKO or CST software. Hence, the IBC-IEq. (Impedance Boundary Condition-Integral Equation) method of CST software has been used to compare and validate the results.

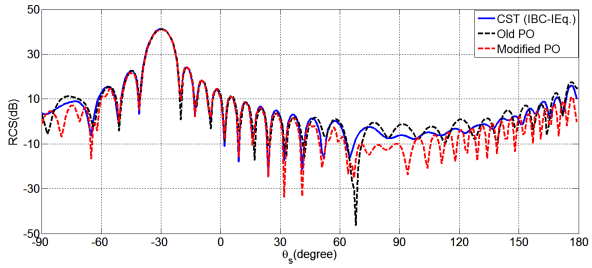

Figure 15: Bistatic RCS for the coated PEC cone in elevation plane that $\theta_i = 30^\circ$, $\phi_i = 0^\circ$ and $\phi_s = 0^\circ$.

TABLE 1
COMPARISON OF THE COMPUTATION TIMES

ature method is used for the upper

STRUCTURE	*PLANE*	*EQS.* (1a) *AND* (1b)	*PROPOSED METHOD*	*FEKO (MLFMM)*	*CST (IBC-IEQ.)*
CYLINDER	AZIMUTH	≈5 min	<2 min	≈420 min	-
CYLINDER	ELEVATION	≈4 min	<1.5 min	≈300 min	-
CONE	AZIMUTH	≈5 min	<2 min	-	≈9 min
CONE	ELEVATION	≈4 min	<1.5 min	-	≈8 min
CONE	MONOSTATIC	≈4 min	<1.5 min	-	≈14 h

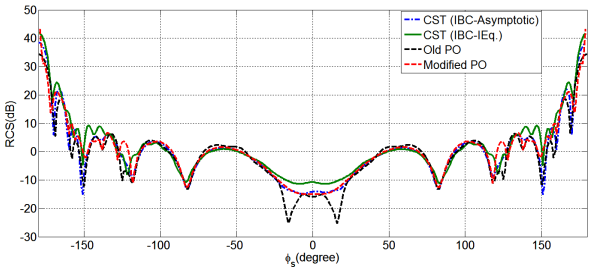

Figure 16: Bistatic RCS for the coated PEC cone in azimuth plane that $\theta_i = 90^\circ$, $\phi_i = 0^\circ$ and $\theta_s = 90^\circ$.

In the last case, the monostatic RCS of a PEC cone coated with a lossy dielectric and with the bottom radius of 2λ, the upper radius of 4λ and the length of 4λ is obtained by the proposed method. The results are shown in Fig. 17. In this case, the dielectric characteristics are $\grave{o}_r = 4$, $\tan\delta = 0.25$ and $t = 0.08\lambda$, and the IBC-IEq. method of CST software has been used to compare and validate the results.

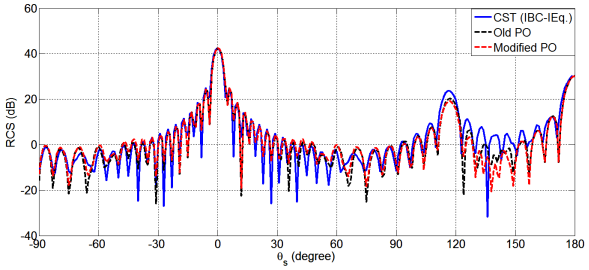

Figure 17: Monostatic RCS for the coated PEC cone at $\phi_i = 0^\circ$ and $\phi_s = 0^\circ$ plane.

By comparing the results of the proposed method and FEKO and CST software, it is obvious that the presented method has good accuracy. As shown in Figs. 9 to 17, (2a) and (2b) calculate RCS more accurately than (1a) and (1b) due to the fact that the traditional PO approximation was modified by the Fresnel reflection coefficients of the dielectric layer. Therefore, using the proposed method, the equivalent current distribution is more accurately calculated than the (1a) and (1b); consequently, more accurate RCS is obtained.

It is worth mentioning that the PO integral of the cone or cylinder is calculated by the SPM. While and lower plates of the cone or cylinder in order to reduce the time of computations compared to the MLFMM and IBC-IEq. techniques.

Table 1 compares the computation times and Table 2 compares the CPU and RAM usage of the proposed formulation, previous formulation, MLFMM and IBC-IEq. to calculate the RCS of the dielectric coated PEC cone and cylinder.

The computer used for this comparison has an Intel Core i5 CPU 2.53 GHz processor and 4 GB of RAM. The proposed technique is considerably faster.

TABLE 2
COMPARISON OF THE CPU USAGE AND REQUIRED RAM.

SOFTWARE	CPU USAGE	RAM USAGE
FEKO (MLFMM)	100%	>3.2 GB
CST (IBC-IEQ.)	50%	>2 GB
MODIFIED PO	25-30%	<0.4 GB

5. CONCLUSION

In this paper, a modified PO approximation based on electric currents is applied to solve coated electrically large objects. The coating layer can be a lossy electric and/or magnetic Radar Absorbing Material (RAM). The traditional PO approximation was modified using the Fresnel reflection coefficients of the RAM.

The results of the proposed method are compared with those of FEKO and CST software using MLFMM and IBC methods, and the previous formulation for PO approximation.

The modified PO integrals of the problem are calculated by the Stationary Phase Method (SPM). However, Gaussian's quadrature method is used to calculate the effect of the upper and lower plates of the cone or cylinder.

The proposed technique reduces significantly the computation time of the simulation compared to FEKO and CST software.

6. ACKNOWLEDGMENT

The authors would like to thank Mr. M. H. Sadrearhami, a PhD student in Electrical Engineering at Sharif Univ. of Tech., for his valuable guidance and advice.

REFERENCES

[1] M. F. Catedra, C. Delgado, and I. G. Diego, "New physical optics approach for an efficient treatment of multiple bounces in curved bodies defined by an impedance boundary condition," *IEEE Transactions on Antennas and Propagation*, vol. 56, no. 3, pp. 728-736, 2008.

[2] F. S. de Adana, I. G. Diego, O. G. Blanco, P. Lozano, and M. F. Catedra, "Method based on physical optics for the computation of the radar cross section including diffraction and double effects of metallic and absorbing bodies modeled with parametric surfaces," *IEEE Transactions on Antennas and Propagation*, vol. 52, no. 5, pp. 3295-3303, 2004.

[3] J. T. Hwang, S. Y. Hong, J. H. Song, and H. W. Kwon, "'Radar cross section analysis using physical optics and its applications to marine targets," *Journal of Applied Mathematics and Physics*, vol. 3, pp. 166-171, 2015.

[4] F. Weinmann, "The Influence of Surface Curvature on High-Frequency RCS Simulations" *The Second European Conference on Antennas and Propagation EuCAP*, Edinburgh, pp. 1-5, Nov. 2007.

[5] C. Corbel, C. Bourlier, N. Pinel, and J. Chauveau, "Rough Surface RCS Measurements and Simulations Using the Physical Optics Approximation" *IEEE Trans. Antennas Propag.*, vol. 61, no. 10, pp. 5155-5165, 2013.

[6] F. Weinmann, "Ray tracing with po/ptd for rcs modeling of large complex objects," *IEEE Trans. Antennas and Propaation.*, vol. 54, no. 6, pp. 1797-1806, 2006.

[7] Y. An, D. Wang, R. Chen, "Improved multilevel physical optics algorithm for fast computation of monostatic radar cross section," *IET Microwaves, Antennas & Propagation*, vol. 8, no. 2, pp. 93-98, 2014.

[8] H. Mohammadzadeh, A. Zeidaabadi-Nezhad, and Z. H. Firouzeh, "Modified physical optics approximation and physical theory of diffraction for rcs calculation of dielectric coated pec," *Antennas and Propagation Society International Symposium* (APSURSI), Orlando-FL, pp. 1896 – 1897, 2013.

[9] A. Noga, "Physical optics approximation for PEC objects coated with lossy material," *2st International Conference in Radioelektronika* 2011, pp. 1-3, 2011.

[10] W. C. Gibson, The Method of Moments in Electromagnetics, Chapman & Hall/CRC and Taylor & Francis Group, 2008.

[11] X. J. Chen , X. W. Shi "Comments on a formulation in radar cross section," *Journal of Electromagnetic Waves and Applications*, vol. 21, no. 15, p. 2389-2394, 2007.

[12] J. J. Stamnes, Waves in Focal Region, IOP Publisher, 1986.

[13] L. P. Felsen, N. Marcuvitz, *Radiation and Scattering of Waves*, IEEE Press, 1994.

[14] J. Perez, M. F. Catedra, "Application of physical optics to the RCS computation of bodies modeled with NURBS surfaces," *IEEE Transactions on Antennas and Propagation*, vol. 42, no. 10, pp. 1404-1411, 1994.

[15] P. C. Lash, "Comparison of computational electromagnetic codes for prediction of low-frequency radar cross section," *Master of Science, Department of Electrical and Computer Engineering, Air Force Institute of Technology*, 2006.

[16] L. M. Brekhovskikh, Waves in Layered Media, 2nd ed., vol. 6, *Academic Press*, 1960.

[17] R. S. Elliott, Antenna Theory and Design, *2nd ed., IEEE Press*, 2003.

[18] C. A. Balanis, Advanced Engineering Electromagnetics, *2nd ed., John Wiley & Sons*, 2012.

[19] D. Klement, J. Preissner, and V. Stein, "Special problems in applying the physical optics method for backscatter computations of complicated objects," *IEEE Transactions on Antennas and Propagation*, vol. 36, no. 2, pp. 228-237, 1988.

BIOGRAPHIES

Hossein Mohammadzadeh was born in Yasouj, Iran, in 1987. He received the B.Sc. degree in Electrical Engineering from Hakim Sabzevary University, Sabzevar, Iran, in 2009 and the M.Sc. degree from Isfahan University of Technology (IUT), Isfahan, Iran, in 2013. His research interests include Electromagnetic Theory, Propagation and Scattering Theory, Antenna and Microwave, and Numerical Techniques. He is currently a researcher at Malek-Ashtar University of Technology.

Abolghasem Zeidaabadi-Nezhad was born in kerman, Iran, in 1961. He received the B.Sc. degree in Electrical Engineering from Kerman Shahid Bahonar University, Kerman, Iran, in 1987 and the M.Sc. and PhD. degrees in Electrical Engineering from Sharif University of Technology, Tehran, Iran, in 1990 and 1997, respectively. His research interests include Propagation and Scattering Theory, Antenna Design, Active and Passive Microwave Circuits, and Semiconductor Devices. He is currently a Faculty Member at the Department of Electrical and Computer Engineering, Isfahan University of Technology.

Zaker Hossein Firouzeh was born in Isfahan, Iran, in 1977. He received the B.Sc. degree in Electrical Engineering from Isfahan University of Technology (IUT), Isfahan, in 1999 and the M.Sc. and PhD. degrees in Electrical Engineering from Amirkabir University of Technology (AUT), Tehran, Iran, in 2002, and 2011, respectively. He was a Research Engineer at Information Communication Technology Institute (ICTI) of IUT from 2002 to 2006. He experienced in design and implementation of antenna, Radar, and wireless communication systems. His current research interests include antenna design and measurements, numerical techniques in electromagnetic, wave propagation and scattering, and EMC/EMI. He is currently a Faculty Member at the Department of Electrical and Computer Engineering, Isfahan University of Technology.